Appl. Phys. A 89, 849–856 (2007)
DOI: 10.1007/s00339-007-4222-3

Applied Physics A
Materials Science & Processing

C. MILIANI[1,✉]
F. ROSI[2]
A. BURNSTOCK[3]
B.G. BRUNETTI[2]
A. SGAMELLOTTI[1,2]

Non-invasive in-situ investigations versus micro-sampling: a comparative study on a Renoirs painting

[1] Istituto CNR-ISTM (Istituto di Scienza e Tecnologie Molecolari), c/o Dipartimento di Chimica, Università degli Studi di Perugia, Via Elce di Sotto 8, 06123 Perugia, Italy
[2] Centro di Eccellenza SMAArt (Scientific Methodologies applied to Archaeology and Art), c/o Dipartimento di Chimica, Università degli Studi di Perugia, Via Elce di Sotto 8, 06123 Perugia, Italy
[3] Courtauld Institute of Art, London, Somerset House, Strand, London,WC2R 0RN, UK

Received: 10 November 2006/Accepted: 25 June 2007

ABSTRACT In this paper, a multi-technique in-situ non-invasive approach has been followed for the study of the materials used for a painting by Pierre-Auguste Renoir, "A woman at her toilette". The study was carried out using five portable spectroscopic techniques, namely X-ray fluorescence, mid-infrared reflectance spectroscopy, near infrared reflectance spectroscopy, and UV-Vis spectroscopy in absorption and emission. The painting was selected as a case study because it was examined in advance of the current investigation using conventional micro-sampling techniques. This provided the opportunity to evaluate potential and limitations of the non-invasive approach to the complex case of the modern painting.

PACS 82.80.GK; 78.70.En; 33.50.Dq

1 Introduction

A great part of international historical patrimony consists of monuments, sculptures, buildings and other art objects in fixed locations. Therefore, technical investigations of the constituent materials of these artefacts require sample-taking or, where this is not permitted, in-situ non-invasive analytical measurements. In addition, in case of movable patrimony, such as easel paintings, ceramics, gems, manuscripts, where sampling is limited or ethically impossible, the mobility of the object from its location to an analytical laboratory may be forbidden for safety or security reasons. As a consequence, analytical and technical study of these works is necessarily limited to in-situ non-invasive approaches.

Due to miniaturization of electronic components and advances in fibre-optic technology improvements in the performance of existing prototypes have been made, that includes the assembly of portable instrumentations with capabilities that are comparable to standard bench equipment. These developments led to the foundation of the European Transnational Access MOLAB, where a mobile laboratory composed of a unique collection of portable equipment has been made available to art-historians, conservators, and conservation scientists for in-situ non-invasive measurements of works of art. There are several significant studies that describe non-invasive analytical investigations carried out on wall paintings and works on panel following a multi-technique in-situ non-invasive approach. Two recent examples are analytical investigations of the painting techniques of Pietro Vannucci called il Perugino, in Perugia, [1, 2] and the identification of Raphaels palette in the Deposizione Baglioni at the Galleria Borghese in Rome [3].

While multi-technique non-invasive in-situ investigations have been carried out on several early paintings, this approach has not so far been applied to the study of modern or contemporary works. Only a few investigations, with limited application of a single technique have been published [4, 5]. Indeed, the materials of modern and contemporary art pose problems that make the non-invasive approach in many cases mandatory, but at the same time more difficult. Due to the good condition of many examples of modern paintings, sampling opportunities are in general more limited than in aged and more damaged works. From the 19th century onwards, paintings became more complex in terms of the number and mixtures of materials used for a single work. From this point of view, impressionism exemplifies a period of dramatic change in patterns of artistic training, practice, and patronage. Newly invented pigments became available, which were sold already mixed in tubes allowing artists to free themselves from traditional studio practice and to render their subject matter more vividly [6].

In this paper, a multi-technique in-situ non-invasive approach has been followed for the study of the materials used for a painting by Pierre-Auguste Renoir, "A woman at her toilette," exhibited in the Courtauld Institute Art Gallery, London. The study was carried out using five portable spectroscopic techniques: X-ray fluorescence (XRF), mid-infrared reflectance spectroscopy (mid-FTIR), near infrared reflectance spectroscopy (near-FTIR), UV-Vis spectroscopy (UV-Vis), and reflectance fluorimetry (RF). The painting was selected as a case study because it was examined in advance of the current investigation using conventional micro-sampling techniques [7]. This provided the opportunity to compare the data obtained and to evaluate potential and limitations of the non-invasive approach to the complex case of a modern painting.

✉ Fax: +390-755855606, E-mail: miliani@thch.unipg.it

"A woman at her toilette", was painted ca. 1919 in Cagnes, towards the end of Renoirs career. From an analytical point of view it represents a challenge incorporating complex mixtures of pigments applied in several layers wet-on-wet.

2 Experimental

The portable equipment for elemental and molecular spectroscopy employed in this work are part of the MOLAB, a mobile laboratory accessible to European scientists through the Eu-ARTECH project, funded by the 6th framework programme (FP).

2.1 *Reflectance mid-infrared (mid-FTIR)*

Spectra were recorded using a portable JASCO VIR 9500 spectrophotometer equipped with a Remspec mid-infrared fibre optic sampling probe. The optical bench is made up of a Midac Illuminator IR radiation source, a Michelson interferometer and a liquid nitrogen cooled MCT-detector. The fiber optic probe is a bifurcated cable containing 19 chalcogenide glass fibers that allow the collection of spectra in the range 4000–900 cm^{-1} at a resolution of 4 cm^{-1}. The width of the investigated area is determined by the probe diameter, which is about 4 mm. The total reflectivity, R, due to the combined diffuse and specular components, is measured using the spectrum from an aluminium mirror plate for background correction. The spectrum intensity was defined as the pseudo absorbance A' where $A' = \log(1/R)$.

2.2 *Reflectance near-infrared (near-FTIR)*

Near infrared spectra were recorded using a portable JASCO VIR 9600 spectrophotometer made up of a halogen lamp as the source, a Michelson interferometer equipped with a $\mathrm{CaF_2}$ beam splitter, and room temperature InGaAs detector. The spectral range is 12 500–4000 cm^{-1} with an energy resolution of 4 cm^{-1}. The spectrophotometer is equipped with a silica glass fiber optic Y sampling probe (2 m-long, 200/300 μm of core) which can remotely measure the reflection of a variety of solid surfaces with a spatial resolution of about 10 mm^2. The spectrum intensity was defined as the pseudo absorbance A' where $A' = \log(1/R)$.

2.3 *Fibre optics reflectance spectroscopy (UV-Vis)*

UV-Vis reflectance spectra were collected using a portable spectrophotometer assembled using the following components: a deuterium tungsten halogen lamp, an Avantes CCD spectrometer (sensitivity 86 photons/counting) in the 250–850 nm range, a bifurcated bundle of quartz fibres and a 45° probe-head. The spectral resolution is about 2 nm and the spatial resolution is about 10 mm^2.

2.4 *Reflectance fluorimetry (RF)*

Micro UV-Vis fluorescence spectra have been recorded using a portable spectrometer equipped with a Nd:YAG laser source with emission at 532 nm. The laser radiation is focused through an optical fiber, with a core diameter of 100 μm, into a JASCO RMP-100 micro probe equipped with an Olympus objective (50 × or 20 ×). The backscattered emission light, is collected (at 180°) by an optical fiber 2 m-long and 200 μm diameter, and led to the polychromator. The compact ORIEL MS125 spectrograph is equipped with a Czerny–Turner polychromator of about 100 mm focal length,with manual scansion. In the spectrograph, the radiation reaches the grating and is then transmitted to a 1024 × 128 pixel CCD ANDOR detector kept at −70 °C by a Peltier cooler.

2.5 *X-ray fluorescence (XRF)*

The XRF spectra were recorded using portable equipment made with a miniaturized X-ray generator EIS P/N 9910, equipped with a tungsten anode and a silicon drift detector (SDD) cooled with a Peltier element. The SDD has a resolution of about 150 eV at 5.9 keV. The portable instrument allows the detection of elements with atomic number higher than silicon ($Z > 14$). The excitation parameters used during the investigations were: voltage of 38 kV and current of 0.05 mA. The acquisition time was 120 s. The distance sample-detector was fixed at 2 cm. The beam diameter under these conditions is 4 mm. A procedure fitting has been employed for calculating the net counts for each element. X-ray emission peaks have been fitted with a Gaussian function and the data expressed as counts per second obtained by dividing the peak area by the acquisition time (120 s). Generally, the K_α emission has been considered for the calculation; only for barium, mercury and lead, were L_α emissions used. As for mercury, its contribution has been estimated by subtracting the signal of tungsten (from X-ray source). In fact, L_β emission of tungsten shows a band shape with a shoulder that falls at the same energy of mercury. The spectra not containing mercury have been employed for determining the contribution of the shoulder to the L_β emission of tungsten. The presence of cobalt has been evaluated by subtracting the contribution of K_β emission of iron. The ratio of K_α/K_β of iron has been

FIGURE 1 Location of the XRF measurements. The spatial resolution due to the beam diameter is about 12 mm^2

calculated in the absence of cobalt and employed for subtracting the iron contribution in the K_α cobalt emission. Low amounts of calcium and potassium in the presence of strong signals of antimony have not been reported, since M emissions of antimony fall at the same energies of calcium and potassium.

The painting ($50.0 \times 56.2\,\mathrm{cm}^2$) was examined in a room of the Courtauld Institute of Art. About seventy areas have been investigated (25 by XRF, 23 by mid-FTIR, 10 by near-FTIR, 5 by UV-Vis, 5 by RF). In Fig. 1, the XRF measurement points are reported. During the measurements the canvas has been simply placed on an easel in front a bench where the equipment was standing.

3 Results

In-situ measurements were carried out using five different analytical techniques, XRF, mid-FTIR, near-FTIR, UV-Vis, and RF. The results describe their integrated use for the identification of the inorganic and organic painting materials, such as the ground layers (visible at one side of the painting), inorganic pigments, and organometallic complex colouring materials known as lakes, organic binding media and coatings.

A mid-infrared spectrum recorded from the ground exposed on the left side of the painting (Fig. 2a) showed that the priming layer is comprised essentially of lead white, identified by the distorted ν_3 reststrahlen band of $\mathrm{CO_3}^-$ at $1400\,\mathrm{cm}^{-1}$. The presence of a drying oil as the binding medium of the priming was suggested by the strong C=O stretching at about $1740\,\mathrm{cm}^{-1}$ partially resolved from $\nu_1 + \nu_4$ of lead white. Calcium sulphate and probably iron oxides (as part of the priming layer) were also detected using mid and near-infrared ($\mathrm{SO_4}^-$ inverted band at $1140\,\mathrm{cm}^{-1}$ and OH combination band at $5170\,\mathrm{cm}^{-1}$) and XRF (about 40 cps for K_α of iron), respectively.

Lead white was identified as white pigment, pure or in mixture. Notably, it was found to be composed mainly by hydrocerussite, as inferred by the presence of both O−H stretching at $3544\,\mathrm{cm}^{-1}$ due to $\mathrm{Pb(OH)_2}$ moiety and the typical shape of combination band of $\nu_1 + \nu_3$ at about 2410 due to $\mathrm{PbCO_3Pb(OH)_2}$ structure (Fig. 2a) [8]. The presence of hydrocerussite was also confirmed by a sharp absorption band in the near-infrared at $6907\,\mathrm{cm}^{-1}$ due to the first overtone of O−H stretching. XRF analysis of the same white areas did not show emission of zinc and barium suggesting that there were no zinc white and barium sulphate in the tube-paint formulation used by Renoir, nor were extenders containing barium or zinc added to the lead white paint.

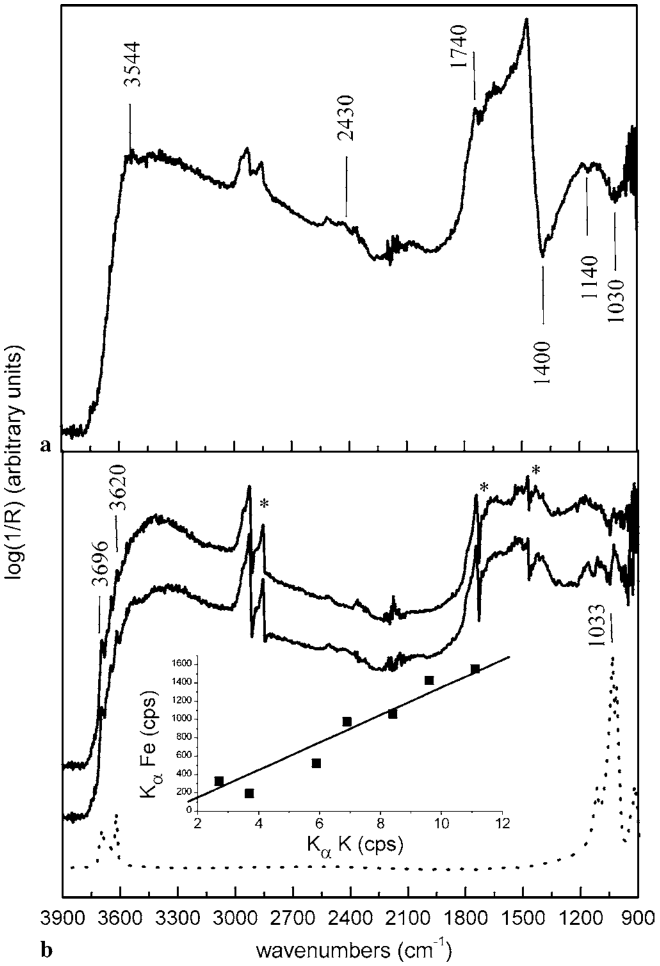

FIGURE 2 (**a**) Mid-FTIR spectrum of priming, signals of lead white and sulphate ($1140\,\mathrm{cm}^{-1}$) are signed; (**b**) mid-FTIR spectra recorded on yellow and red areas compared with a standard of kaolin (*dot line*, from the IRUG database in transmission mode), *stars* indicate derivative features of wax, *insert* reports the plot Fe vs. K counts for areas containing kaolin

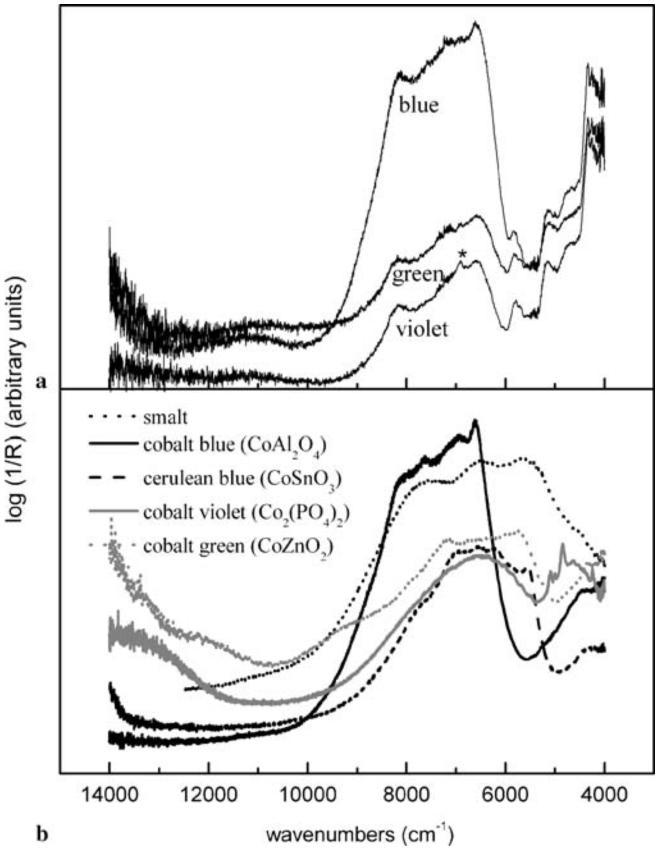

FIGURE 3 (**a**) Near-FTIR reflectance spectra of blue, green and violet coloured areas containing Co (Table 1); (**b**) reference spectra of cobalt-based pigments. *Stars* indicates the first overtone of O−H stretching at $6907\,\mathrm{cm}^{-1}$ due to lead white

Element	K	Ca	Cr	Mn	Fe	Co	Zn	Hg	Pb	Sr	Sb
Emission line	K_α	K_α	K_α	K_α	K_α	K_α	K_α	L_α	L_α	K_α	K_α
01_blue	–	6.4	–	6.0	24.6	1076.5	–	19.7	725.5	7.1	–
02_purple	–	9.4	–	–	27.6	110.3	–	96.5	821.8	11.7	–
03_red	–	–	3.7	–	93.1	6.9	44.7	63.8	786.5	10.2	17.0
04_red	–	–	2.2	–	149.4	10.0	103.5	155.8	736.6	11.9	35.4
08_red	8.4	30.8	9.3	–	1059.8	–	33.6	24.3	807.1	7.4	24.8
09_red	6.9	33.5	7.2	–	978.2	–	–	25.4	784.5	5.7	16.3
11_red	–	–	11.5	–	72.7	6.4	77.2	113.3	979.8	13.3	32.0
12_red	–	–	27.4	–	129.1	12.4	88.2	209.1	825.8	11.5	55.2
18_red	9.6	50.5	10.7	11.2	1422.2	–	20.6	11.4	1331.9	21.8	–
22_red	2.7	15.3	5.0	–	326.4	–	–	178.3	822.9	19.2	–
7_pink	–	–	–	16.3	–	11.3	128.1	61.2	989.1	10.1	24.9
10_green	–	–	361.9	–	232.6	120.3	53.8	24.5	902.5	6.7	23.8
13_green	–	–	1449.1	–	195.3	431.1	58.5	15.0	654.9	6.5	38.4
26_green	3.7	28.4	650.6	–	192.4	208.9	44.4	25.8	1283.2	10.4	24.6
5_yellow	–	–	6.7	–	519.6	–	172.3	–	794.0	5.2	66.7
6_yellow	–	–	–	–	123.6	5.4	320.1	–	737.1	7.3	119.7
14_yellow	11.1	–	144.3	–	1553.7	–	218.9	20.1	1014.9	6.6	103.3
16_yellow	–	–	4.6	4.9	138.0	–	655.6	–	988.2	–	456.1
23_yellow	–	6.5	–	–	393.5	–	18.6	10.2	1104.1	3.8	–
24_yellow	–	–	–	3.8	379.8	–	324.4	15.3	1074.4	4.9	117.5
25_yellow	5.9	9.3	7.0	–	522.7	–	25.9	30.5	1376.1	9.0	–
15_white	–	5.3	5.2	–	10.2	–	–	10.4	1720.5	6.2	–
17_white	–	–	–	5.4	9.2	–	–	–	1744.7	–	-
19_black	–	82.9	–	–	38.6	–	88.5	16.7	1507.9	20.0	48.0
20_black	–	72.3	9.1	–	56.4	5.0	57.1	95.0	1529.6	24.1	35.3
21_ground	–	78.7	–	–	43.4	–	18.0	–	1506.3	28.1	–

TABLE 1 XRF results obtained on the Renoir‘s painting expressed as counts/s. Points of analysis are reported in Fig. 1

Blue, purple and green areas were found to be particularly rich in cobalt with a K_α emission signal ranging from about 1000 cps to about 100 cps (Table 1). Near-infrared spectra recorded on the same Co rich areas showed a well-structured electronic absorption in the range 6500–8500 cm^{-1}. The spectral features of the near-infrared electronic absorption allowed the chemical structure of cobalt coordination compounds to be characterized, that distinguishes smalt (alkali glass containing Co^{2+}), cobalt blue ($CoAl_2O_4$), cerulean blue ($CoSnO_3$), cobalt violet ($Co_2(PO_4)_2$) and cobalt green ($CoZnO_2$). The near-infrared transition of cobalt-based pigments is due to the *d–d* electronic transition of cobalt(II) tetrahedrally coordinated and it is structured into three sub-bands by the Jahn–Teller effect. In Fig. 3, near-infrared spectra of different cobalt-based pigments are compared with spectra recorded from blue, purple and green areas of the Renoirs painting. They show three well resolved sub-bands at about 6610, 7230 and 8150 cm^{-1} revealing that cobalt is always present as the blue $CoAl_2O_4$. [9]. The spectrum recorded on the violet area shows also a band at 6907 cm^{-1} due to the first overtone of O−H stretching of lead white, already discussed above.

XRF measurements on yellow and green areas indicated the presence of antimony, suggesting the use of a lead antimony yellow, also know as Naples yellow. Counts of antimony correlated well with those for zinc, as illustrated by Fig. 4 that plots the cps for Sb K_α against the cps for Zn K_α ($\text{Zn}/\text{Sb} = 1.49 \pm 0.08$ with a correlation rate $R = 0.95$).

This finding strongly suggested that the Naples yellow was prepared following the recipes published by Dingler on the Polytechnishes Journal (1828) that reports Pb_3O_4 (8 oz.), Sb (12 oz.) and ZnO (4 oz.) as reagents [10]. According to historical documentation, Renoir abandoned the use of chrome yellow (the newly invented $PbCrO_4$) in favour of the more traditional Naples yellow in the 1880s [6]. In this work, the use of lead antimonate was confirmed, while in some yellow areas chromium was also detected, always mixed with Naples yellow. There is no correlation between Cr and Sb counts, hence the presence of chrome yellow might be interpreted as a choice of the painter and not as an additive to Naples yellow supplied in a single tube.

Values for chromium are particularly high in green painted areas, ranging from about 360 to 1450 cps (K_α emission). This can be ascribed to the use of chrome yellow in mixture with cobalt blue and also to an addition of viridian green ($Cr_2O_3 \cdot 2H_2O$), that is known to be widely used by impressionist painters to enhance the green nuance of the paint hue [6].

Red and purple-coloured areas were characterized by the presence of mercury that gives a positive identification of vermilion (Table 1). UV-Vis spectra generally confirmed the presence of vermilion showing an S-shaped feature with an inflection point around 580 nm (Fig. 5) typical of the band-to-band electronic transition of mercury sulphide [11]. Spectra recorded on red-coloured areas of paint that had a low count for mercury (8_red, 09_red and 18_red in Table 1) showed different features, with a well-structured absorption band having maxima at 516 and 548 nm and a shoulder at 480 nm. The same areas also showed an intense fluorescence emission at about 600 nm strongly suggesting the presence of an anthraquinone lake [12]. UV-Vis spectral properties in absorption and emission of red coloured areas, high or low in elemental mercury, are summarized in Fig. 5.

Some yellow and red areas were also characterized by the presence of iron and potassium with a constant ratio Fe K_α/K K_α of about 150 ± 15 (see insert in Fig. 2b, correlation rate $R = 0.99$). In the same areas mid-FTIR spectroscopy revealed the presence of kaolinite, a clay mineral with the chemical composition $Al_4[Si_4O_{10}](OH)_8$. The diagnostic bands for kaolin clay are two sharp OH stretchings at about $3620\,cm^{-1}$, assigned to internal OH groups, and near $3700\,cm^{-1}$, from internal surface OH groups [13]. In the reflectance mode acquisition, both OH-stretching band are well resolved from the matrix absorption. Kaolinite, known also as China clay, is reported to have Mg and K as minor elements [14] and therefore it is possible to ascribe the XRF signals of iron and potassium on red and yellow areas with a mixture of kaolinite and iron oxides.

Dark red and grey areas also showed the presence of bone black identified by the presence of a sharp features at $2010\,cm^{-1}$ related to the phosphate content of the pigment [3, 8] as illustrated in the infrared spectrum of Fig. 6. On some dark areas traces of manganese were detected by XRF, possibly due to addition of MnO_2.

Analysis of the organic materials suggested that the paint is covered by a natural wax, characterized by clear mid-infrared features, at 2900–3000 (CH stretching, very strong), at 1730 (C=O stretching, strong) and at (1470 C–C bending, strong), all showing a derivative shape as usually occurs for wax measured in reflectance and not for drying oil as binder. These features in derivative mode are visible, for example, on spectra 2b (here indicated with asterisks) and 6, while they are not present on spectrum 2a as collected from an area of the priming layer from the edge of the canvas where only siccative oil is visible. The presence of natural wax made it

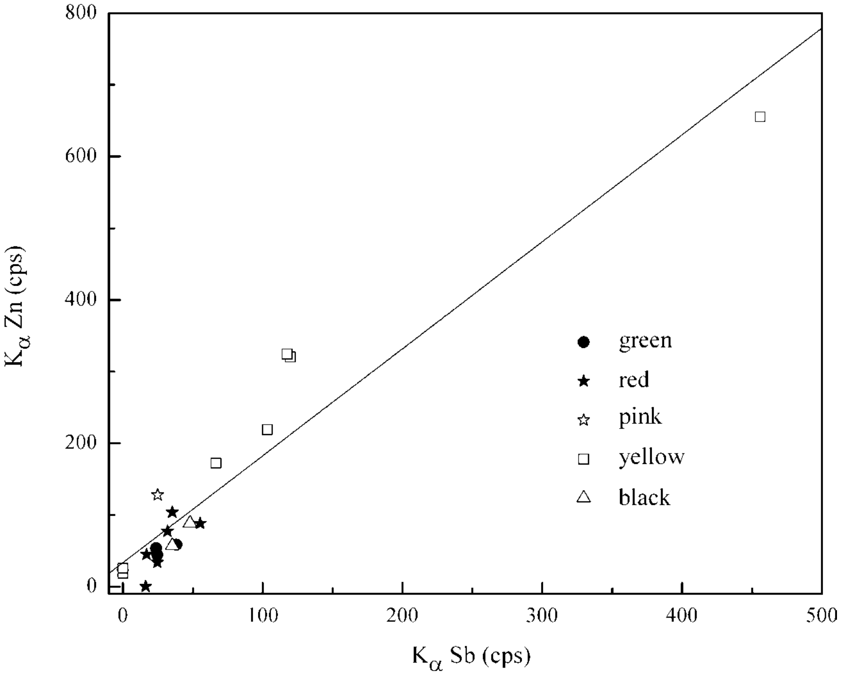

FIGURE 4 Plot of Zn K_α cps vs. Sb K_α cps, the linear fit has an $R = 0.95$

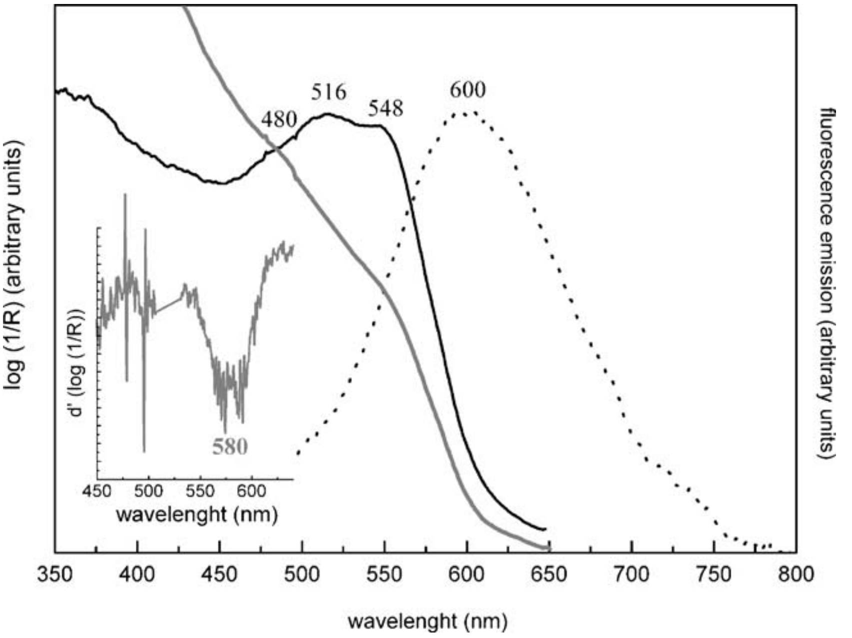

FIGURE 5 UV-Vis absorption and emission spectra recorded on red areas: *grey line* – absorption spectrum from Hg rich red, the *insert* shows its first derivative spectrum, *black line* – absorption spectrum from a Hg poor red, *dot line* – emission spectrum from the same Hg poor red ($\lambda_{exc.} = 532$ nm)

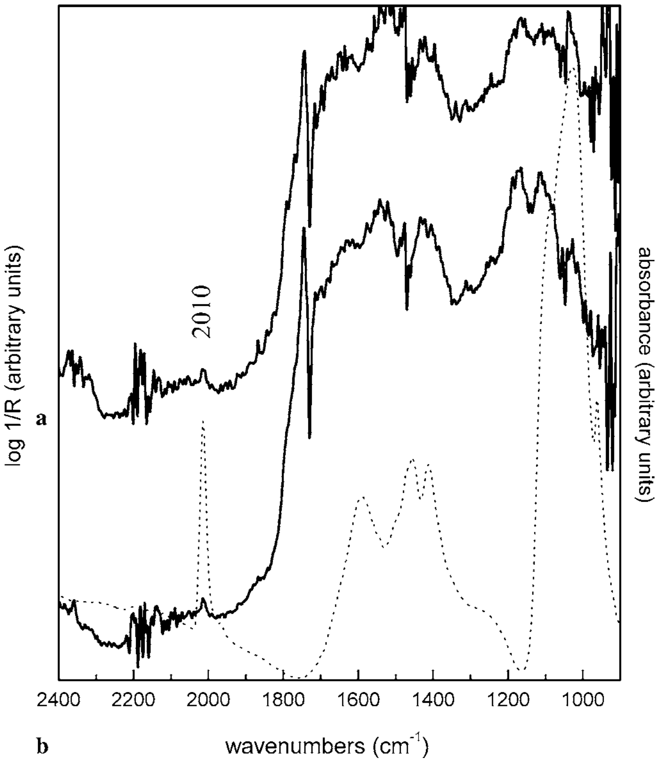

FIGURE 6 Mid-FTIR reflectance spectra recorded on grey (**a**) and dark (**b**) areas. At 2010 cm^{-1} a sharp and weak absorption specific of bone black is visible. The reference spectrum is from the IRUG database (transmission mode) is reported as *dot line*

impossible to use the non-invasive method employed here for characterization of paint binding media, that has previously been identified using GC-MS as linseed oil mixed with other drying oils or nut oil, and also with starch on some specific areas [7]. Nevertheless, wax was identified using non-invasive FTIR while it was not characterised using GC-MS, probably because the wax was removed as part of the preparation of the sample for the analysis, or because the procedures adopted were not suitable for the analysis of natural waxes, that require hydrolysis under specific conditions prior to GC-MS analysis [15].

The Renoir canvas appeared to be unvarnished due to the matt appearance of the surface. It was thought to have survived unvarnished because no reports on treatment are available since its acquisition by Samuel Courtauld, who bought the picture directly from Vollard, Renoirs dealer in 1922 [6]. It is possible that the natural wax was applied at the Courtauld as part of an early, undocumented conservation treatment. Alternatively wax may have been incorporated as part of the paint medium, either by the artist to achieve particular paint effects or by the paint manufacturer. This has been already suggested in a previous micro-destructive FTIR study [16] carried out in a painting by Toulouse Lautrec in which the authors have characterized the presence of a mixture of beeswax and drying oil. In the present study that employed mid-FTIR spectroscopy in reflectance mode, it was not possible to distinguish between the use of wax as a coating or as a binder, and analyses of a cross-section by micro-FTIR, or of selective micro-sampling by GC-MS might provide the necessary spatial resolution.

4 Discussion

Renoirs "A woman at her toilette (1919)" is a characteristic example of the pastel-toned fulsome women that the artist painted at the end of his career. The opportunity to study this painting using a range of non-invasive methods allowed an evaluation of the potential and limitations of the selected methods, with regard to the problems posed by the materials and techniques used by this impressionist painter.

The results obtained from non-invasive analyses are discussed in comparison with results from a micro-sampling approach including SEM-EDS for the identification of inorganic pigments, GC-MS and FTIR for the identification of binders, and HPLC for the characterization of the organic components of lake pigments. The measurements were carried on eleven micro-samples taken from the edges of the painting and are reported elsewhere [6].

This study demonstrated that the quantity and the quality of the information that can be obtained using the present in-situ non-invasive multi-technique approach make it an important and valuable method for the technical study of the complex impressionist painting materials. With regard to the identification of pigments, the comparison of the results with those previously obtained through micro-sampling shows a remarkable convergence as summarized in Table 2. The identification of pigments on cross sections, carried out using a combination of optical microscopy and elemental analysis by SEM-EDS, included lead white, cobalt blue, chrome yellow (with composition PbZnCr), Naples yellow, viridian green, red earth, vermilion and bone black [6]. In addition, red lake was identified by HPLC. The non-invasive methods used in the present study were sufficient for the identification of all these pigments with the exception of viridian green pigment.

In spite of the substantial agreement of the data obtained using the different methods, some minor differences were found. These include the interpretation of the Zn content in yellow areas, and the characterisation of viridian green. XRF analysis attributed the zinc to a compound added to Naples yellow pigment on the basis of a good correlation between Sb and Zn counts, while the interpretation of elemental analysis using SEM-EDS ascribed the presence of elemental Zn to a yellow zinc chromate pigment, containing Pb, Zn, and Cr (probably in solid solution, as characterised using XRD on other samples [17]). The identification of viridian green that was uncertain on the basis of XRF data was more confidently concluded from the presence of crystals composed only by Cr in SEM-EDS examinations. The identification of viridian green was achieved on a micro-sample taken from dark green area behind the woman in correspondence with XRF point analysis 13_green (see Fig. 1), where in fact the counts of Cr emission line were the highest (about 1450 cps for the K_α emission). A third difference between the methods was that non-invasive analysis characterised the presence of kaolin, added to extend red earth pigment.

In evaluating the performance of the non-invasive methods, it is relevant to note that possible limitations are not related to low sensitivity or low specificity of the exploited techniques. As an example, the energy resolutions of the equipment are relatively good: 4 cm^{-1} for mid and near-FTIR, 150 eV for XRF, 2 nm for UV-Vis both in absorption

Colour	Non-invasive analyses	Micro-destructive analyses [7]
White (pigment and primer)	lead white (mainly hydrocerussite)	lead white
Blue	cobalt blue	cobalt blue
Yellow	Naples yellow with Zn addiction, chrome yellow, mixture of kaolinite with iron oxides	Naples yellow, chrome yellow with Zn addiction
Green	chrome yellow + cobalt blue and/or viridian	viridian
Red	cinnabar, antraquinone lake, mixture of kaolinite with iron oxides	cinnabar, red lake, red earth
Dark red, gray	bone black with Mn-oxides	bone black
Organic material	wax, oil	linseed oil mixed with other drying oils or nut oil, starch

TABLE 2 Comparison between results obtained by the non-invasive and micro-destructive approach

and in emission. The more significant limitation of the method is the restricted spectral range offered by the non invasive set-up compared with bench laboratory equipments. Currently available chalcogenide optical fibers absorb the mid-infrared radiation under 900 cm^{-1} precluding the characterisation of metal oxides and chromates (as for example viridian green chromium oxide) used as pigments or extenders. In addition, the commonly used X-ray generators do not allow the detection of elements with atomic number lower than 14, thus not permitting the identification of some pigments as the French ultramarine blue (a sodium aluminium silicate cage containing sulphur anions) used by impressionist painters [6].

Another limitation of the non-invasive method arises from the so-called matrix effect, always present when working directly on the paint surface. It is well know that the matrix effect is particularly limiting in XRF investigations where every layer of the painting stratigraphy screens X-rays both of excitation and of fluorescence leading to the loss of proportionality between intensity and concentration. Nevertheless, signal intensity can be used to obtain relative comparison among points having similar bulk composition and stratigraphy, as exploited in the discussion regarding the presence of Naples yellow, chrome yellow and viridian green. In infrared spectroscopies the matrix effect results in a possible overlap of absorption bands that can not be properly resolved. However, in spite of this inconvenience, exploiting specific diagnostic features sometimes different from those commonly used in transmission mode, it possible to identify several functional groups, as for example carbonates from $\nu_1 + \nu_3$ combination band, clays from OH-stretchings, or cyano compounds from CN stretching.

The great advantage of non-invasive methods is that no contact or sampling is necessary and therefore all the areas of the painting can be examined without any limitation. This overcomes the main limitation of the micro-sampling approach, where data is drawn from a single sampling site that is determined not by choice or interest but by the opportunity to sample close to an edge of the painting or the edge of a damaged area. Moreover, the large number of measurements possible using the non-invasive approach can provide statistical validation of the data, so that even small features, such as OH-stretching bands of kaolin in IR, or correlation between Sb and Zn and between Fe and K in XRF, can be considered reliable.

Another advantage of the non-invasive approach lies in the possibility of acquisition of complementary information on the same wide areas, thanks to the exploiting of several different analytical techniques. As an example, regarding the identification of Co-based pigments the weakness of XRF in-situ analysis of not being sensitive to low atomic number atoms, such as Al, is overcome by the specificity of the near-infrared spectroscopy for Co^{2+} d–d transitions that are strongly affected by the host crystal lattice.

The analytical problems are more complicated for the range of organic compounds used for painting, including lake pigments, binding media and coatings, because the spectroscopic techniques employed for characterization of these materials provide only data on functional groups and are therefore less specific for these compounds. This is true not only for the portable non-invasive equipment used in this study but for the same equipment used in a laboratory. Precise identification of organic molecules from paintings is easily achievable only by chromatographic methods on micro-samples. Despite that, this work demonstrated that a non-invasive spectroscopic characterization of the organic components of the painting layer could be of great benefit for enhancing the capabilities of micro-destructive chromatographic analysis. The presence of a single type of red lake, probably an anthraquinonic dye, has been highlighted using simply UV-vis spectroscopy both in absorption and in emission mode. This finding could properly guide a minimized sampling to collect only one representative sample to be analysed by HPLC.

Surprisingly, the presence of natural wax has been revealed by mid-FTIR, probably it is a restoration varnish not visible to the naked eye, nor documented on conservation reports. This result could be useful to optimize not only the sampling, but also the sample treatment and the chromatographic procedures.

In conclusion, from the results of the present study it is possible to establish an appropriate protocol for the analytical study of paintings, that transcends the present investigation. The first step might consist of a preliminary in-situ examination using complementary non-invasive techniques, that offer the opportunity for extensive analysis of the painting, giving substantial information on the composition of the main materials and their distribution over the surface; the second step would consist of a limited and selective sample-taking to give answers to the questions that still remain open. Obviously, micro-sampling remains essential when it is important to examine stratification of materials or to precisely identify organic compounds.

ACKNOWLEDGEMENTS The work has been carried out through the support of the EU within the 6th Framework Programme (Contract Eu-ARTECH, RII3-CT-2004-506171). A.B. gratefully acknowledges all the staff of the MOLAB Transnational Access.

REFERENCES

1 C. Miliani, F. Rosi, I. Borgia, P. Benedetti, B.G. Brunetti, A. Sgamellotti, Appl. Spectrosc. **61**, 293 (2006)

2 B.G. Brunetti, C. Seccaroni, A. Sgamellotti, *The Painting Technique of Pietro Vannucci, called the Perugino* (Nardini Editore, Rome, 2004)

3 A. Roy, M. Spring, *Raphaels Painting Technique: Working Practices before Rome* (Nardini Editore, Rome, 2006)

4 M. Bacci, A. Casini, C. Cucci, M. Picollo, B. Radicati, M. Vervat, J. Cult. Herit. **4**, 329 (2003)

5 F. Zieske, The Book and Paper Group Annual 14 (Washington AIC Book and Paper Group Annual, 1995), p. 105

6 D. Bomford, J. Kirby, J. Leighton, A. Roy, *Art in the Making: Impressionism* (The National Gallery, London, in association with Yale University Press, New Haven, London, 1990)

7 A. Burnstock, K.J. van der Berg, J. House, in: *Art Matters, Netherlands Technical Studies in Art* (Waanders, Zwolle, 2005), Vol. 3, p. 47

8 C. Miliani, C. Ricci, F. Rosi, M. Vagnini, B.G. Brunetti, A. Sgamellotti, submitted to Vib. Spectrosc.

9 M. Bacci, M. Picollo, Stud. Conserv. **41**, 136 (1996)

10 A. Roy, *Artists‘ Pigments* (National Gallery of Art, Washington in association with Oxford University Press, New York, London, 1993)

11 M. Bacci, Sens. Actuators B **29**, 190 (1995)

12 C. Miliani, A. Romani, G. Favaro, J. Phys. Org. Chem. **13**, 141 (2000)

13 M.J. Wilson, Clay *Mineralogy: Spectroscopic and Chemical Determinatice Methods* (Chapman & Hall, London, 1994)

14 N. Eastaugh, V. Walsh, T. Chaplin, R. Siddall, *Pigment Compendium* (Elsevier, Butterworth-Heinemann, Amsterdam, Boston, 2004)

15 A. Andreotti, I. Bonaduce, M.P. Colombini, G. le Gautier, F. Modugno, E. Ribechini, Anal. Chem. **78**, 4490 (2006)

16 F. Wrubel, F. Casadio, *Conservation at the Art Institute of Chicago* (Art Institute of Chicago in association with Yale University Press, Newhaven, London, 2005)

17 A. Burnstock, C. Jones, G. Cressey, Z. Kunstt. Konserv. **1**, 74 (2003)